

Genome-wide identification of key genes responding to salt stress in *Populus alba*

Xiu-Yan Bian

Chinese Academy of Forestry

Yuan Xue

Chinese Academy of Forestry

Peng-Fei Jiang

Chinese Academy of Forestry

Qing-Yin Zeng

Chinese Academy of Forestry

Yan-Jing Liu

yan.jing.liu@163.com

Chinese Academy of Forestry

Research Article

Keywords: *Populus alba*, salt stress, physiological characteristic, transcriptome, biochemical function

Posted Date: May 23rd, 2024

DOI: <https://doi.org/10.21203/rs.3.rs-4395721/v1>

License:  This work is licensed under a Creative Commons Attribution 4.0 International License.

[Read Full License](#)

Additional Declarations: No competing interests reported.

Abstract

Background

The molecular mechanism of forest trees responding to salt stress remains poorly understood. As a fast-growing and widely adapted tree species, *Populus alba* is planted in the world. Understanding the molecular mechanism of *P. alba* responding to salt stress is helpful to improve the yield of *P. alba* artificial forest in salinized land.

Results

This study investigated the phenotypic and physiological characteristics of *P. alba* seedlings under 300 mM NaCl stress. After seven days of salt stress, the leaves of *P. alba* turned yellow and fell off. Whether under normal growth conditions or salt stress, CAT activities in roots were significantly higher than that in leaves. The root viability of *P. alba* decreased significantly within 2 h of salt treatment, but gradually increased after 2 h of salt treatment. Intercellular CO₂ concentration of leaves of *P. alba* increased significantly after 72 h of salt treatment, while other photosynthetic parameters decreased significantly after 72 h of salt stress. Chlorophyll *a* and chlorophyll *b* in leaves of *P. alba* decreased gradually after 9 h of salt stress. The ratio of Na⁺/K⁺ in roots and leaves of *P. alba* gradually increased after 1 and 2 h of salt stress, respectively. ABA and cytokinin contents in roots and leaves of *P. alba* under salt stress were increased significantly. Time-series transcriptomes of roots, stems, leaves, and apical buds of *P. alba* under NaCl stress were analyzed. Based on gene expression, physiological and biochemical data in *P. alba* under salt stress, we performed weighted gene co-expression network analysis. Thirty-two candidate key genes of *P. alba* responding to salt stress were identified. Twenty-four candidate key genes showed salt tolerance in *Saccharomyces cerevisiae*. Especially for the four genes (*Poalb01G005590*, *Poalb16G007310*, *Poalb01G036340*, and *Poalb06G010440*), each exhibited strong tolerance to different kinds of salt stress.

Conclusion

The results of this study provide a new insight into the molecular mechanism of trees responding to salt stress.

Background

Soil salinization is an increasingly serious problem in the world. High salt concentration has serious effect on the growth and development of crops, and will eventually lead to a decrease in crop yield [1, 2]. In addition to natural soil salinity, irrigation and climate change exacerbate the threat. Climate change may occur through sea level rise or increase evaporation during the drought period [3]. Now, salt stress is one of the main environmental factors that affect the growth of crops [4, 5]. Soil salinization results in

growth inhibition, development change, metabolic adaptation change, and ion sequestration or exclusion in crops [6]. Salt stress also can disturb physiological processes in crops, especially photosynthesis [7]. Soil salinization will increase the osmotic pressure of soil solution, which will result in difficulty for crops to absorb water from the soil. When the soil salinization is serious, it will lead to the leakage of water from the roots of crops, and eventually result in wilt or die [8, 9].

Salt tolerance of different plant species is varied. For example, citrus and tomato have low tolerance, while cotton and barley have high tolerance [9]. According to the ability of salt tolerance, plants can be classified into halophytes and glycophytes. Halophytes can naturally grow in or even depend on high NaCl environment. For example, species of *Atriplex* and *Salicornia* can grow in an environment of up to 1000 mM NaCl [10]. Most crops are glycophytes, their growth may be severely inhibited by the low Na⁺ concentration, which means they need fresh water. Glycophytes are difficult to survive or even die in salinized soil. Thus, optimizing glycophytes to make them more salt tolerant is a strategy to increase crop yield on salinized agricultural land [1, 11]. The advantage of halophytes is that, in addition to the basic salt tolerance mechanism shared with glycophytes, they have greater osmotic adjustment ability and ion metabolism strategies, such as the redistribution of Na⁺, K⁺, and ion contents in different tissues and cell compartments of plants, as well as the regulatory mechanisms of relative transporters [1].

Populus alba is a deciduous tree belonging to Salicaceae. This taxon is widely distributed in Europe, and in Central Asia [12]. *P. alba* grows rapidly, and has excellent characteristics such as cold resistance and pest resistance. As a fast-growing tree and a good biomass product, white poplar is included in the European Program of Forest Genetic Resources [13]. The natural population of *P. alba* is widely distributed in the northwest of China, mainly in Xinjiang province, where over one-third of the cultivated land is facing salinization hazards [14]. Analyzing and improving the salt tolerance of *P. alba* and expanding their planting area in native distribution areas is of great value for forest breeding. High-quality sequencing of *P. alba* genome has been available. In this study, we investigated the phenotypic and physiological characteristics of *P. alba* seedlings under 300 mM NaCl stress. And transcriptome of *P. alba* seedlings in different tissue at different salt stress time were sequenced. The co-expression network of genes related to salt tolerance traits was constructed by WGCNA (Weighted Correlation Network Analysis). A total of 32 candidate key genes of *P. alba* responding to salt stress were identified, and their salt tolerance was verified in yeast. The results of this study provide a new insight into the molecular mechanism of trees responding to salt stress.

Results

Phenotype of *P. alba* seedlings under salt stress

In this study, within one day of salt stress treatment, no significant phenotypic changes were observed in *P. alba* seedlings (Fig. 1). After three days of salt stress treatment, the mature leaves of *P. alba* turned yellow, and the tips and edges of leaves became dry and curled (Fig. 1A). The tips and margins of the leaves at the top of the *P. alba* were dry and slightly curled after three days of salt stress treatment

(Fig. 1B). After seven days of salt stress treatment, the leaves of the whole plant turned yellow and the mature leaves were partially shed. After 11 days of salt stress treatment, the leaves of the whole plant turned yellow and withered.

POD, CAT activities and MDA content in roots and leaves of *P. alba* seedlings under salt stress

Compared with normal growth seedlings, POD activities in seedling roots were significantly increased after salt stress for 1 h (independent sample *t*-test, $P < 0.01$). Compared with other salt stress treatment time points, POD activity in seedling roots was the lowest at 72 h of salt stress (independent sample *t*-test, $P < 0.01$), and was the highest at 264 h of salt stress (independent sample *t*-test, $P < 0.01$) (Fig. 2A).

We found that CAT activities in seedling roots were higher than that in leaves under normal growth conditions or salt stress (independent sample *t*-test, $P < 0.01$) (Fig. 2B). Compared with other salt stress time points, CAT activity in seedling roots was the highest at 12 h of salt stress (independent sample *t*-test, $P < 0.01$).

Compared with normal growth seedlings, MDA content in seedling leaves significantly increased after 2 h of salt stress treatment (independent sample *t*-test, $P < 0.05$) (Fig. 2C). Compared with other salt stress time points, MDA content in seedling leaves was the highest at 264 h of salt stress (independent sample *t*-test, $P < 0.05$).

Root viability of *P. alba* seedlings under salt stress

The root viability of *P. alba* was significantly decreased at 1 and 2 h after salt stress (independent sample *t*-test, $P < 0.01$) (Fig. 3). Compared with other salt stress time, the root viability of *P. alba* seedlings was the lowest at 2 h of salt stress (independent sample *t*-test, $P < 0.01$), and then gradually increased. Compared with other salt stress time, the root viability of *P. alba* seedlings was the highest at 168 h under salt stress.

Photosynthetic parameters of *P. alba* seedlings under salt stress

We determined the photosynthetic parameters of the third leaf in *P. alba* under normal growth conditions and salt stress. Compared with normal growth conditions, the significant changes of net photosynthetic rate (Pn), stomatal conductance (Cond) and transpiration rate (Tr) were not observed within 12 h of salt stress. After 12 h of salt stress, values of Pn, Cond and Tr decreased gradually, and decreased to zero at 264 h (Fig. 4). Compared with normal growth conditions, the intercellular CO₂ concentration (Ci) of leaves of *P. alba* did not change significantly within 72 h of salt stress. However, after 72 h of salt stress, Ci value increased significantly. The maximum quantum efficiency of photosystem II (PSII) photochemistry (Fv/Fm) of leaves of *P. alba* gradually decreased after 24 h of salt stress, and then decreased to zero at 264 h (Fig. 4). Values of the ABS/RC (maximal energy fluxes for absorption per reaction center), DI₀/RC (maximal energy fluxes for energy dissipation per reaction center), ET₀/RC (maximal energy fluxes for electron transport rate per reaction center), and TR₀/RC (maximal energy

fluxes for trapping per reaction center) were significantly decreased after 168 h of salt stress, and were decreased to zero at 264 h. The contents of chlorophyll *a*, chlorophyll *b* and carotenoid in leaves of *P. alba* seedlings gradually decreased after 9 h of salt stress (independent sample *t*-test, $P < 0.01$) (Fig. 4).

Na⁺ and K⁺ contents in roots and leaves of *P. alba* seedlings under salt stress

This study determined the concentration of Na⁺ and K⁺ and the Na⁺/K⁺ ratio in the roots and leaves of *P. alba* under normal growth and salt stress (Fig. 5). Compared with the normal growth conditions, the significant change of K⁺ concentration in the roots of *P. alba* was not observed under salt stress during 0 ~ 24 h, but after 24 h of salt stress, the K⁺ concentration in the roots was gradually decreased. After 264 h salt stress, the K⁺ concentration in *P. alba* roots decreased by 0.57 fold compared to normal conditions.

After 1 h of salt stress, the content of Na⁺ in the roots of *P. alba* was increased gradually. Under salt stress for 264 h, the Na⁺ concentration in the roots of *P. alba* increased by 6.00 folds compared with that under normal growth conditions. The ratio of Na⁺/K⁺ in the roots of *P. alba* was increased gradually after 1 h of salt stress. Under salt stress for 264 h, the ratio of Na⁺/K⁺ in the roots of *P. alba* increased by 15.22 folds compared with that under normal growth conditions.

The K⁺ content in the leaves of *P. alba* increased significantly during the 1 ~ 12 h of salt stress. The Na⁺ content in *P. alba* leaves gradually increased after 2 h of salt stress. After 264 h for salt stress, the Na⁺ content was increased by 489.22 folds compared with normal growth conditions. The ratio of Na⁺/K⁺ in *P. alba* leaves gradually increased after 2 h of salt stress.

The increase rate of Na⁺ content in leaves was much higher than that in roots, while the K⁺ content retained stable in leaves and decreased in roots. These lead to a sharper increase in the Na⁺/K⁺ ratio of leaves than that of roots. These physiological observations, including Na⁺ transport from root cells to xylem and higher levels of K⁺ retention, have been found in halophytes [9].

Hormone content in roots and leaves of *P. alba* seedlings under salt stress

In this study, we determined content changes of endogenous hormones in the roots and leaves of *P. alba* under salt stress (Fig. 6, Table S1 and Table S2). Compared with 0 h, contents of SL (strigolactone), IAA (indole acetic acid), GA₁ (gibberellin A₁), GA₃ (gibberellin A₃), GA₄ (gibberellin A₄), GA₇ (gibberellin A₇), mT (meta-Topolin), 6-BA (6-benzyladenine), tZ (trans-Zeatin), and DZ (dihydrozeatin) did not change significantly in the roots of *P. alba* under salt stress (independent sample *t*-test, $P > 0.05$). Compared with 0 h, contents of ABA (abscisic acid), SA (salicylic acid), iP (N^6 -(Δ^2 -isopentenyl)-adenine), pT (para-Topolin), oT (ortho-Topolin), and cZ (cis-Zeatin) in the roots of *P. alba* were increased significantly at a certain time point of salt stress, but contents of JA (jasmonic acid), ETH (ethylene), and K (kinetin) were decreased significantly at a certain time point of salt stress (independent sample *t*-test, $P < 0.05$).

Compared with 0 h, contents of OPC-4 (3-oxo-2-(2-(z)-pentenyl)-cyclopentane-1-butyric acid) and OPDA (cis(+)-12-oxophytodienoic acid) in the roots of *P. alba* were decreased after 3 h of salt stress, while the contents of iPR (N6-isopentanyladenosine), KR (kinetin riboside), pTR (para-Topolin riboside), and cZR (cis-Zeatin riboside) were the highest at one of salt stress time points. Compared with 0 h, SAG (salicylic acid 2-o- β -glucoside) in the roots of *P. alba* was increased after 72 h of salt stress, while JA-Ile (jasmonoyl-L-isoleucine) was decreased after 3 h of salt stress (Table S1).

Contents of SL, JA, GA₁, GA₃, GA₄, 6-BA and K in the leaves of *P. alba* did not show changes significantly compared with 0 h (independent sample *t*-test, $P > 0.05$), while, contents of ABA, SA, ETH, IAA, GA₇, iP, pT, mT, oT, cZ, tZ and DZ in the leaves showed changes significantly after 72 h of salt stress (independent sample *t*-test, $P < 0.05$). Compared with 0 h, contents of salicylic acid derivative SAG, abscisic acid derivative ABA-GE (ABA-glucosyl ester), cytokinin derivative oT9G (ortho-Topolin-9-glucoside), cZROG (cis-Zeatin-O-glucoside), and tZOG (trans-Zeatin-o-glucoside) in the leaves of *P. alba* were increased after 72 h of salt stress, while the contents of cytokinin derivatives DHZROG (dihydrozeatin-O-glucoside) and mT9G (meta-Topolin-9-glucoside) were decreased after 72 h of salt stress (Table S2).

Transcriptome of *P. alba* seedlings under salt stress in different tissues and different time points

The time-series transcriptome of roots, stems, leaves, and apical buds of *P. alba* under salt stress were detected. Sequencing of all examined tissues at 11 time points under salt stress resulted in 8.08 billion raw reads (Table S3). After quality control, a total of 7.3 billion clean reads and 106.63 Gb clean bases were obtained (Table S3). The average proportion of these clean reads mapped to the reference genome of *P. alba* was 95.78% (Table S3). Among them, the average proportion of clean reads with uniquely mapped position in reference genome was 91.02% (Table S3). Subsequently, we used these clean reads with uniquely mapped position in reference genome to perform gene expression analysis. In addition, the transcriptomic data of three biological repeats within each group were highly correlated, indicating stable and reliable results (Fig. S1, $R^2 > 0.96$).

Differential genes in different tissues of *P. alba* seedlings under salt stress

During the 1 ~ 24 h of salt stress, the number of up-regulated differentially expressed genes (DEGs) in the roots of *P. alba* was greater than down-regulated (Fig. 7). On the contrary, after 72 h of salt stress, the number of down-regulated DEGs in the roots of *P. alba* was greater than that of up-regulated. In the leaves and apical buds of *P. alba* under salt stress, the DEGs number was increased significantly after 72 h. In the stems of *P. alba* under salt stress, the DEGs number was increased significantly after 168 h.

We randomly selected three DEGs (*Poalb16G007310*, *Poalb08G012240*, and *Poalb18G005570*) for RT-qPCR validation (Fig. S2). The RT-qPCR results showed, compared with 0 h, *Poalb18G005570*, *Poalb16G007310*, and *Poalb08G012240* were specifically expressed in stems, leaves, and apical buds during the salt stress, respectively, which was consistent with the transcriptome results.

Identification of key candidate genes responding to salt stress in roots of *P. alba* seedlings

Based on transcriptome-based gene expression data, and the physiological and biochemical data in *P. alba* roots under salt stress, we used WGCNA (Weighted Correlation Network Analysis) software to perform weighted gene co-expression network analysis (Fig. 8). A total of 61 modules related to phenotype data were identified. The modules whose absolute value of correlation coefficient between phenotype and module eigengene was greater than 0.8 were MEblue, MEmidnightblue, METurquoise, and MEDarkslateblue. These four modules were mainly related to Na⁺, Na⁺/K⁺ and phytohormone contents (Fig. 8A).

Modules METurquoise, MEblue, MEmidnightblue, and MEDarkslateblue contained 7506, 4784, 298, and 64 genes in roots of *P. alba*, respectively. GO enrichment showed that the genes in METurquoise module were mainly related to histone modification, chromatin organization, and vesicle-mediated transport (Fig. S3). The genes in MEblue module were mainly related to cell wall biogenesis, cell division, cytokinesis, and organelle fission (Fig. S3).

Only six genes from module MEblue (*Poalb04G009630*, *Poalb09G004310*, *Poalb02G001570*, *Poalb10G017000*, *Poalb16G000560*, and *Poalb18G012460*) and five genes from module METurquoise (*Poalb01G003930*, *Poalb01G005590*, *Poalb13G004180*, *Poalb02G018040*, and *Poalb06G007330*) exhibited sustained differential expression at all time points under salt stress. Among these 11 DEGs, except for *Poalb06G007330*, the other 10 genes were up-regulated expression under the salt stress in the roots of *P. alba* (Fig. 8B). Co-expression network analysis showed that the *P. alba* ANN1, bHLH112, CC1/2, KT2, PGDH1/3, SKOR/GORK, CCAOMT1, NAC019, and HKT1 showed co-expression patterns with the six sustained differentially expressed genes in the MEblue module (Fig. 8C). In the METurquoise module, the five sustained differentially expressed genes showed co-expression patterns with bHLH112, SOS2, SOS3, SOS1, SAG29, OSCA1, FER, KT2, and AKT1 (Fig. 8D). Sequence analysis showed that these genes belonged to 11 gene families, which included RanBP2-type zinc finger family, calcium-binding EF-hand family, small heat-shock proteins (smHSPs) family, SIAMESE/SIAMESE-RELATED (SIM/SMR) family, QWRF motif-containing protein family, aldo-keto reductase (AKR) family, leucine-rich-repeat receptor-like kinase (LRR-RLK) family, cinnamoyl-CoA Reduce (CCR) family, sugars will eventually be exported transporters (SWEETs) family, thioredoxin reductase family, and TEOSINTE BRANCHED 1 and CYCLOIDEA, PCF1 (TCP) family (Table 1).

Table 1
Key candidate genes respond to salt stress in *P. alba* seedlings.

Gene ID	Family Name
Poalb06G007330	RanBP2-type Zinc Finger (ZnF) Family
Poalb02G018040	Calcium-binding EF-hand Family
Poalb09G004310	Small Heat-shock Proteins (smHSPs) Family
Poalb10G017000	SIAMESE/SIAMESE-RELATED (SIM/SMR) Family
Poalb13G004180	QWRF motif-containing Protein Family
Poalb16G000560	Aldo-keto Reductase (AKR) Family
Poalb18G012460	Leucine-rich-repeat Receptor-like Kinase (LRR-RLK) Family
Poalb01G003930	Cinnamoyl-CoA reductase (CCR) Family
Poalb01G005590	Sugars Will Eventually be Exported Transporters (SWEETs) Family
Poalb02G001570	Thioredoxin Reductase Family
Poalb04G009630	TEOSINTE BRANCHED 1, CYCLOIDEA, PCF1 (TCP) Family
Poalb02G006720	Unknown
Poalb16G007310	FISSION1 (FIS1) Family
Poalb01G001990	Plant P-type H ⁺ -ATPase (P-ATPase) Family
Poalb09G006800	Lateral Organ Boundaries Domain (LBD) Family
Poalb12G010830	Type 2C Protein Phosphatases (PP2Cs) Family
Poalb18G005570	Raffinose Synthase (RS) family
Poalb01G036340	Vascular-related Unknown Protein Family
Poalb03G010320	MAPK kinase kinase (MAP3K) Family
Poalb02G006200	Unknown
Poalb04G005680	Unknown
Poalb06G010440	HXXD-type Acyltransferase Family
Poalb07G008970	Unknown
Poalb09G012950	Cytochrome P450 Family
Poalb08G012240	Metallo-phosphoesterase Family
Poalb11G009160	Calcium-binding EF-hand Family
Poalb14G005890	Phospholipase D (PLD) Family

Gene ID	Family Name
Poalb01G007070	Ethylene-responsive Factor (ERF) Family
Poalb06G004370	Ethylene-responsive Factor (ERF) Family
Poalb18G011550	Ethylene-responsive Factor (ERF) Family
Poalb02G003950	Cytochrome P450 Family
Poalb11G014910	NAM, ATAF1/2, CUC2 (NAC) Family

Identification of key candidate genes responding to salt stress in leaves of *P. alba* seedlings

Based on transcriptome-based gene expression data, and the physiological and biochemical data in leaves of *P. alba* under salt stress, we used WGCNA software to perform weighted gene co-expression network analysis (Fig. 9). A total of 43 modules related to phenotype data were identified. The modules whose absolute value of correlation coefficient between phenotype and modules was greater than 0.8 were MEpurple, MEblack, MEsteelblue, MEdarkred, MElightgreen, MEpink, MERoyalblue, METurquoise, MEGreen, and MEblue (Fig. 9A).

The genes in these 10 modules were all related to plant phytohormone. In addition, the METurquoise module was also related to MDA, Chl *a*, Chl *a/b*, Ci, Pn, Cond, Tr, Na⁺, and Na⁺/K⁺ ratio. The MEGreen module was related to the phenotypic traits of Ci, Fv/Fm, TRo/RC, ETo/RC, etc. The MEblue module were related to Chl *a/b*, Pn, Cond, Tr, MDA, Na⁺, and Na⁺/K⁺ ratio.

The modules of METurquoise, MEblue, MEblack, MEGreen, MEpink, MERoyalblue, MEpurple, MEsteelblue, MElightgreen, and MEdarkred contained 11795, 6853, 618, 834, 600, 167, 380, 62, 173 and 135 genes in leaves of *P. alba*, respectively. Because METurquoise and MEblue contained more DEGs, it indicated that these two modules may be more important in response to salt stress in leaves of *P. alba*.

GO enrichment showed that the genes in the METurquoise module were mainly related to photosynthesis, cytoplasmic translation, and ribosome biogenesis (Fig. S4). The genes in MEblue module were mainly related to cell wall biogenesis, organelle fission, and mitotic cell cycle process (Fig. S4).

The module of METurquoise did not contain any genes, which were DEGs at any time point under salt stress. While, the module of MEblue contained two genes (*Poalb02G006720* and *Poalb16G007310*), that were DEGs at different time points under salt stress. These two genes were highly connected with the key genes (such as SOS1, SOS2 and SOS3) in the known molecular regulation mechanism of salt stress (Fig. 9C). Sequence analysis showed that *Poalb02G006720* was an unknown functional gene, and *Poalb16G007310* belonged to FISSION1 (FIS1) family (Table 1). These two genes were up-regulated in the leaves of *P. alba* under salt stress (Fig. 9B).

Identification of key candidate genes responding to salt stress in stems and apical buds of *P. alba* seedlings

Because of the lack of phenotypic data of apical buds and stems, we used another method to identify the key candidate genes responding to salt stress. Firstly, according to the functional data in the public papers, we identified 531 genes related to salt stress from *Arabidopsis thaliana*. Using these 531 genes as templates, the genome of *P. alba* and *P. trichocarpa* was searched by TBLASTN software. All protein sequences of each gene family obtained from *P. alba*, *P. trichocarpa*, and *A. thaliana* were used to construct a phylogenetic tree. On the phylogenetic tree, the *P. alba* gene closest to the salt stress gene in *A. thaliana* was considered to be related to salt stress. Based on this principle, 1215 homologous genes to salt stress genes in *A. thaliana* were found in the genome of *P. alba* (Table S4). Secondly, we regarded the DEGs obtained in apical buds or stems at different stress time points as a set. K-means algorithm divided this set into 10 clustering subsets (Fig. S5). We calculated the total number of homologous genes related to salt stress in each clustering subset in *P. alba*. The clustering subsets with the first and second largest number of salt stress homologous genes were selected for further analysis. In these two subsets, the genes that exhibited sustained differential expression under salt stress were considered as key candidate genes.

Based on above principle, this study identified six key candidate genes (*Poalb12G010830*, *Poalb18G005570*, *Poalb01G001990*, *Poalb01G036340*, *Poalb03G010320* and *Poalb09G006800*) responding to salt stress in *P. alba* stems (Fig. 10A). The expression of these six genes was up-regulated in *P. alba* stems under salt stress.

Thirteen key candidate genes (*Poalb02G003950*, *Poalb09G012950*, *Poalb14G005890*, *Poalb08G012240*, *Poalb11G014910*, *Poalb01G007070*, *Poalb04G005680*, *Poalb11G009160*, *Poalb06G004370*, *Poalb18G011550*, *Poalb06G010440*, *Poalb02G006200*, and *Poalb07G008970*) responding to salt stress were found in *P. alba* apical buds (Fig. 10B). The expressions of *Poalb14G005890*, *Poalb08G012240*, *Poalb01G007070*, *Poalb04G005680*, *Poalb11G009160*, *Poalb06G004370*, *Poalb18G011550*, *Poalb06G010440*, *Poalb02G006200*, and *Poalb07G008970* were up-regulated in *P. alba* apical buds under salt stress, while *Poalb02G003950* and *Poalb09G012950* were down-regulated. The expression of *Poalb11G014910* was down-regulated at 72 h and was up-regulated at other time points.

Functional verification of key candidate genes of *P. alba* responding to salt stress

Based on the above analysis, we identified 32 candidate genes from the roots, leaves, stems, and apical buds of *P. alba* responding to salt stress (Table 1). Among these 32 genes, *Poalb13G004180* was a pseudogene. Thus, this study first cloned the remaining 31 candidate genes. Except for *Poalb02G006720*, 30 candidate genes were cloned successfully. For heterologous gene expression, we subcloned the coding regions of these 30 genes into yeast vector pYES2 and transferred them into competent cells of *Saccharomyces cerevisiae* BY4741.

Compared with the negative control, the yeasts that overexpressed *Poalb01G003930*, *Poalb02G018040*, *Poalb10G017000*, *Poalb04G005680*, *Poalb01G007070* or *Poalb18G011550* genes could not survive under the stress of 1.8 M sodium chloride, 2.0 M potassium chloride, or 4.0 M sorbitol, while the yeasts that overexpressed other 24 genes showed tolerance to these stresses (Fig. 11). The yeasts that overexpressed *Poalb01G001990*, *Poalb09G006800*, *Poalb14G005890*, *Poalb11G009160*, *Poalb02G001570*, *Poalb07G008970* or *Poalb02G003950* could only survive under the stress of sodium chloride, but could not under the sorbitol and potassium chloride stress. The yeasts that overexpressed *Poalb06G007330*, *Poalb12G010830*, *Poalb04G009630*, *Poalb11G014910* or *Poalb06G004370* could survive under the stress of sodium chloride and sorbitol. The yeasts that overexpressed *Poalb18G012460*, *Poalb08G012240*, *Poalb02G006200*, *Poalb09G012950*, *Poalb03G010320* or *Poalb18G005570* could survive under the stress of sodium chloride and potassium chloride. The yeasts that overexpressed *Poalb01G005590*, *Poalb16G007310*, *Poalb01G036340*, or *Poalb06G010440* could survive under the stress of sodium chloride, potassium chloride and sorbitol.

Discussion

In the long-term evolution of plants, effective survival strategies have been developed to adapt to salinized soils. Many studies on plant responding to salt stress focused on crops, while molecular mechanism of forest tree responding to salt stress remains poorly understood. In this study, based on analysis of biochemical, physiological, and transcriptome traits, we identified the key candidate genes of *P. alba* involved in salt stress response.

Low concentration of reactive oxygen species (ROS) can be used as a signal to activate salt stress response. However, high concentration of ROS is harmful to protein, lipids, DNA, and carbohydrates, etc. High concentration of ROS can result in oxidative stress and even cell death [15, 16]. Plants have effective enzymatic and non-enzymatic antioxidant defense systems to remove ROS. Catalase (CAT) is an important enzyme in plant active oxygen scavenging system, which can scavenge excessive active oxygen free radicals [17]. In this study, whether under normal growth conditions or under salt stress conditions, the CAT activities in *P. alba* roots were much higher than that in leaves (Fig. 2). This indicated that the roots of *P. alba* may have stronger ability or requirement to scavenge active oxygen. One possible explanation is that, as an organ that plants directly contact with soil, roots are more susceptible to salt stress. Roots need stronger antioxidant capacity to cope with the oxidative stress caused by salt stress.

Malondialdehyde (MDA) is one of the products of membrane lipid peroxidation. In plants, salt stress will increase the degree of membrane lipid peroxidation in leaves [18]. And a large amount of MDA will be produced [19]. High concentration of MDA will disrupt the structure and integrity of cell membrane, and lead to the increase of cell membrane permeability [19, 20]. This study found that the MDA content in leaves was higher than that in roots under salt stress (Fig. 2). This indicated the root of *P. alba* had better cell membrane integrity than the leaf under salt stress.

In this study, we found that the stomatal conductance was decreased significantly after 24 h of salt stress. After 168 h, the stomatal conductance value was zero. High salt concentration will lead to increased water loss and enhanced transpiration of leaves. To maintain water balance, plants will close stomata and reduce water loss. Salt stress will decrease the stomatal conductance of leaves and limit the entry of carbon dioxide into leaves.

Similarly, we found that the contents of chlorophyll *a* and chlorophyll *b* continued to significantly decrease after 24 h of salt stress. Chlorophyll *a* is the key pigment in the process of photosynthesis, which is mainly located in the chloroplast membrane. Its main function is to capture photons and convert them into electronic energy, thus triggering the reaction of photosynthesis. Chlorophyll *a* can absorb blue light and red light, which play a key role in different stages of photosynthesis [21]. Chlorophyll *b* is mainly located in the photosynthetic complex of chloroplasts. Chlorophyll *b* can absorb light energy and transfer it to chlorophyll *a*, thus enhancing the efficiency of photosynthesis [22]. Decreasing of chlorophyll *a* and chlorophyll *b* contents indicated that photosynthesis of *P. alba* was affected after 24 h of salt stress.

Further, a slight decrease in intercellular CO₂ concentration (Ci) of leaves of *P. alba* was found during 24 ~ 72 h salt stress. During this period, although the photosynthetic system was affected by salt stress, the seedlings were still able to maintain stable maximum photosynthetic efficiency (Fv/Fm), and the limited closure of stomata reduced the value of Ci. After 72 h salt stress treatment, the value of Fv/Fm began to decrease, indicating that the accumulated high salinity was disrupting the photosynthetic system. Although no significant differences were detected, ABS/RC, TR₀/RC, and DI₀/RC showed an upward trend after 72 h of salt stress treatment, while the values of ET₀/RC showed a temporary decrease at 72 h. This seems to be a compensation for the decrease in photosynthetic rate by a higher photosynthetic activity of a single reaction center in *P. alba* seedlings. However, excessive higher energy absorption than the energy utilization may also cause damage to the photosystem. Subsequently, the significant decrease in photosynthetic efficiency led to a significant increase in Ci.

Plant hormones play important roles in various environmental stresses including responding to salt stress [5]. In this study, compared with normal growth conditions, ABA content in roots and leaves of *P. alba* under salt stress was increased significantly (Fig. 6). ABA, as an important plant hormone, can connect the development processes and plant defense signal transduction under salt stress [23]. Salt stress will decrease the water absorption of plants, resulting in osmotic stress. The increase of endogenous ABA content will lead to stomatal closure to regulate water balance and osmotic homeostasis [24]. This osmotic pressure regulation function is one of the important functions of ABA-mediated plant salt stress response, which helps plants to maintain water balance under salt stress and reduce the harm of salt stress to plants.

In this study, compared with normal growth conditions, we found that cytokinin (CKs) content in roots and leaves of *P. alba* under salt stress was increased significantly (Fig. 6). As plant hormones that influence growth and the stimulation of cell division, CKs play key roles in plants' response to salt stress

[25]. CKs can affect the absorption, transport and distribution of ions in plants and reduce the damage of salt ions to plant cells. For example, CKs can promote the excretion of Na^+ and the absorption of K^+ , and maintain the ion balance inside and outside the cell [26]. Salt stress will lead to a large number of reactive oxygen species and free radicals in plants, which will cause oxidative damage to plant cells. CKs can improve the antioxidant ability of plants and reduce the occurrence of oxidative damage [27].

In this study, we identified 32 key candidate genes in response to salt stress in *P. alba*. Biochemical functions for salt tolerance of 30 candidate key genes were verified in *Saccharomyces cerevisiae* (Fig. 11). Among these 30 key candidate genes, we found that there were 24 genes, and the over-expressed yeast strains of each gene showed different degrees of tolerance. Our results indicated that these genes played important roles in the response to salt stress of *P. alba*. Especially, there are four genes (*Poalb01G005590*, *Poalb16G007310*, *Poalb01G036340*, and *Poalb06G010440*), and each gene had strong tolerance to different kinds of salt stress (e.g. sodium chloride, potassium chloride and sorbitol).

Under salt stress, the expression of *Poalb16G007310* gene was up-regulated at every time point in the leaves of *P. alba*. *Poalb16G007310* gene belongs to FISSION1 (FIS1) protein family. In *Arabidopsis*, FIS1A and FIS1B play rate-limiting and partially overlapping roles in promoting the fission of peroxisomes and mitochondria [28]. Under salt stress, *Poalb16G007310* may play an important role in the division of peroxisome and mitochondria in *P. alba* leaves. Peroxisome is a small organelle with many oxidation reactions, and its division and proliferation are induced under various stress conditions including salt stress [29].

Under salt stress, the expression of *Poalb06G010440* gene was up-regulated at every time point in the apical buds of *P. alba*. *Poalb06G010440* gene belongs to HXXD-type acyltransferase family. HXXD-type acyltransferase family proteins are a kind of enzymes involved in fatty acid and lipid metabolism, which play an important role in plant growth, development and coping with abiotic stress [30, 31]. These proteins participate in the synthesis and modification of lipids by catalyzing acyl transfer reaction, thus affecting the composition and function of plant cell membranes [32, 33]. Salt stress will lead to the disorder of ion balance in plant cells, and then cause damage to cell membrane. The HXXD-type acyltransferase family proteins can affect the composition and properties of cell membrane and improve the stability of cell membrane by regulating the synthesis and modification of lipids, thus helping plants to better cope with salt stress. In addition, previous study shows that HXXD-type acyltransferase family proteins are also involved in the synthesis and signal transduction of plant hormones, such as SA [34]. The HXXD-type acyltransferase family proteins may regulate the response of plants to salt stress by affecting the synthesis and signal transduction of plant hormones.

Under salt stress, the expression of *Poalb01G005590* gene was up-regulated at every time point in the roots of *P. alba*. *Poalb01G005590* gene belongs to Sugars Will Eventually be Exported Transporters (SWEETs) family. SWEETs are one-way sugar transporters that promote the diffusion of sugar molecules on cell membrane. SWEETs play a role in many physiological functions in plants, including phloem

loading, senescence, and respond to abiotic and biotic stresses [35]. In *Arabidopsis*, the homologous gene of *Poalb01G005590* is *At5g13170* (*SAG29*). *SAG29* is also named as plasma membrane-localized MtN3 protein. *Arabidopsis* *SAG29* can regulate cell viability under high salt conditions. This gene is mainly expressed in aging tissues and induced by osmotic stress of ABA-dependent pathway. When this gene is overexpressed in *Arabidopsis*, transgenic plants show accelerated senescence and hypersensitive phenotype to salt stress [36].

Conclusion

In this study, the phenotypic and physiological characteristics of *P. alba* seedlings under 300 mM NaCl stress were investigated. The time-series transcriptome of roots, stems, leaves, and apical buds of *P. alba* under NaCl stress were sequenced and analyzed. 32 candidate key genes of *P. alba* responding to salt stress were identified. 24 candidate key genes showed salt tolerance in yeast. Four candidate key genes had strong tolerance to different kinds of salt stress. The results of this study provide a new insight into the molecular mechanism of trees responding to salt stress.

Materials and Methods

Plant growth conditions and salt stress treatment

Micro-propagated plants of *Populus alba* were grown on 5% agar-solidified 1/2 MS (Murashige and Skoog) with 1.5% sucrose and 1 mg/L NAA (Naphthaleneacetic acid) under the pH ranging from 5.8 to 6.0. The growth chamber conditions were set as follows: 24 °C, 16 h of light per day and light density of ~ 6000 lux. After four weeks of micropropagation, the plants (~ 10 cm shoot length) were selected and transferred into 10 cm (diameter) × 15 cm (height) plastic pots containing substrates with a ratio of 5:3:2 for peat soil, vermiculite, and perlite. The young seedlings were grown under the growth conditions of 21 °C, 16 h of light per day and light density of ~ 6000 lux for three months. During the growth period, these cultured seedlings were watered twice a week.

In the present study, three-month-old seedlings of *P. alba* were respectively subjected to 0 and 300 mM NaCl for 0, 1, 2, 3, 6, 9, 12, 24, 72, 168 and 264 h. Roots and the third leaves of seedlings under normal growth conditions and salt stress were then harvested for physiological and biochemical characteristics. Additionally, contents of phytohormone-related traits in the third leaves and roots and transcriptome sequencing assays of roots, stems, the third leaves, and apical buds were only conducted under salt stress.

Measurement of root viability, membrane lipid peroxidation and enzymatic activities

Root samples of 66 *P. alba* seedlings divided into two groups treated with 0 and 300 mM NaCl were respectively selected to quantify root viability, which was performed in three biological replicates per

time point. Root viability was tested with triphenyl tetrazolium chloride (TTC) method proposed by Steponkus and Lanphear [37].

For peroxidase (POD) and catalase (CAT) activities, the third leaves and roots of 88 *P. alba* seedlings divided into two groups treated with 0 and 300 mM NaCl were respectively conducted in four biological replicates per time point. CAT and POD activities were measured following by the kit manuals (Jiancheng Bio, Nanjing, China).

For malondialdehyde (MDA) contents, the third leaves and roots of 88 *P. alba* seedlings divided into two groups treated with 0 and 300 mM NaCl were respectively performed in four biological replicates per time point. The MDA contents were conducted by the methods as described by Yang et al. [38].

Measurement of phytohormone-related traits

In total, 99 seedlings of *P. alba* divided into 11 groups were treated with 300 mM NaCl. Roots and leaves of every three individual seedlings at each time point were respectively mixed into one replicate. There were three replicates at every time point. Roots and leaves at different salt stress time were respectively used to quantify phytohormone contents. Along with their precursors, storage and metabolites, the quantification of endogenous abscisic acid (ABA), salicylic acid (SA), jasmonic acid (JA), indole-3-acetic acid (IAA), gibberellic acid (GA), strigolactone (SL), ethylene (Eth), and cytokinins (CKs) was performed using HPLC-MS/MS platforms (MetWare, WuHan, China).

Quantification of Na and K contents

We respectively selected 88 *P. alba* seedlings divided into two groups respectively treated with 0 and 300 mM NaCl to measure Na⁺ and K⁺ contents. The roots and leaves were dried in an oven at 65 °C until a constant weight were reached. The dried samples were then grounded to powder by a shaker instrument (TissueLyser II, Retsch, QIAGEN). Samples were weighted, followed by placed in 68% HNO₃ (ratio of samples to HNO₃ was 0.1 g/8 mL) for 24 h at room temperature and were finally digested using a microwave system (MARS, CEM, USA). The digested samples were diluted to 50 mL with distilled water, and Na⁺ and K⁺ contents were determined by inductively coupled plasma optical emission spectrometer (7700 Series ICP-MS, Agilent, USA). The leaf and root samples at per time point were conducted in four biological replicates, respectively. Na⁺/K⁺ ratio was subsequently calculated.

Quantification of photosynthetic pigment levels

The third leaves of 88 *P. alba* seedlings divided into two groups respectively treated with 0 and 300 mM NaCl were ground by liquid nitrogen and soaked in 80% acetone to extract photosynthetic pigments, and the extracts were centrifuged at 5300 × g for 10 min. The absorbance of the supernatant was then read at 470, 645 and 663 nm using the EvolutionTM 300 UV-Vis Spectrophotometer (Thermo). The levels of

chlorophyll *a* (Chl *a*), chlorophyll *b* (Chl *b*) and carotenoid (Car) concentrations were calculated using methods described by Bruinsma [39]. Finally, the ratio of Chl *a* and Chl *b* (Chl *a/b*) was caculated. Four biological replicates were carried out and each replicate was tested for six technical repeats per time point.

Measurement of photosynthetic parameters

Photosynthetic parameters of the third leaves in *P. alba* seedlings under salt stress and normal growth conditions were measured.

Chlorophyll fluorescence parameters were measured according to the manufacturer's instructions using the FluorPen FP100 (FluorCam, Czech Republic), such as Fv/Fm (maximum quantum efficiency of photosystem II (PSII) photochemistry), PI_{ABS} (performance index (potential) for energy conservation from photons absorbed by PSII to the reduction of intersystem electron acceptors), ABS/RC (maximal energy fluxes for absorption per reaction center), TR₀/RC (maximal energy fluxes for trapping per reaction center), ET₀/RC (maximal energy fluxes for electron transport rate per reaction center)), DI₀/RC (maximal energy fluxes for energy dissipation per reaction center). Nine biological replicates were measured per time point.

The Li-6400 portable photosynthesis system (Li-Cor, Lincoln, NE, USA) equipped with a red/blue LED light source. All measurements were executed at 21 °C with a photon flux density of 1200 µmol m⁻² s⁻¹, and at a CO₂ concentration of 400 µmol mol⁻¹. These gas exchange parameters included the net photosynthetic rate (Pn), stomatal conductance (Cond), transpiration rate (Tr), and intercellular carbon dioxide concentration (Ci). Four biological replicates were measured per time point.

Transcriptome sequencing and analysis

For time-series transcriptome sequencing, 66 *P. alba* seedlings were selected. Four different tissues, including roots, stems, leaves, and apical buds, were respectively harvested in six biological replicates. A total of 132 samples in three biological replicates were subjected to transcriptome sequencing. The rest three biological replicates were used for backup. RNA isolation, library construction and paired-end sequencing were carried out at Biomarker Technologies (Beijing, China).

Raw reads were edited by discarding adaptor sequences, empty reads and reads with unknown or low-quality bases using fastp v0.23.2 [40]. Clean reads were mapped to the *P. alba* genome v2.0 (unpublished) using HISAT2 v2.2.1 [41]. The reads uniquely mapped to the genome were chosen for further analysis. Transcript assembly and quantitation of these transcriptomic data were evaluated using StringTie v2.1.3b [42], and FPKM (fragments per kilobase of transcript per million fragments mapped) values were calculated to measure the expression levels. Differential expression analysis was performed using DESeq2 package [43]. The criterion of *q*-value of 0.05 and an expression value of | \log_2 |fold change |>1 were selected as the threshold to characterize differentially expressed genes (DEGs) [44].

Histogram of DEGs was drawn by ggplot2 package [45]. Gene expression clustering was constructed by STEM v1.3.13 [46]. GO (Gene Ontology) enrichment was analyzed using clusterProfiler package v3.18.0 [47]. Heatmaps of gene expression levels were carried out by pheatmap package v1.0.12 [48].

Identification of genes related to salt stress in *P. alba*

The genome files from *Arabidopsis thaliana* (TAIR10) and *P. trichocarpa* (v4.1) were downloaded from Phytozome v13 [49].

Full-length amino acid sequences of these gene families related to salt stress in *A. thaliana* were selected as the seeds and searched using the TBLASTN program with parameters including -evalue $1e^{-5}$ and -outfmt 6 in genomes of *P. alba* and *P. trichocarpa*, respectively. The obtained sequences were further verified via NCBI Conserved Domain Database tool and mapped back to amino acid sequences of *Arabidopsis* using BLASTP program. These identified protein sequences were all aligned using the MAFFT v7.475 program [50] and conducted to construct maximum-likelihood (ML) algorithm phylogenetic trees using IQTREE v1.6.12 [51] under the reliability of a bootstrap test with 1000 replicates.

Co-expression network analyses

Genes, except for whose sum of read counts at different stress time points equal to zero, were subjected to Weighted Gene Co-Expression Network Analysis (WGCNA) software [52] for further analysis. Based on the correlation between physiological and biochemical data and module eigengene (ME), the associated heat map was created. Modules with a correlation greater than or equal to 0.8 and *P*-value less than 0.05 were selected in the module-trait associations. Then, the co-expression networks were constructed for candidate genes responded to salt stress identified from roots and leaves in *P. alba*, and were visualized using VisANT v5.0 [53].

Vector construction and stress tolerant transformants in yeast

To characterize candidate genes in response to salt stress in *P. alba*, the full-length coding sequences were respectively subcloned into yeast shuttle vector pYES2. The primers used to construct the expression vector were listed in Table S5.

The pYES2 (empty vector control) and plasmids containing these candidate genes were transformed into yeast BY4741 competent cells, respectively. These yeast cells were then grown in the SD-U liquid medium with rotation speed of 220 rpm at 29 °C for 12 h and their OD₆₀₀ values were gradually diluted with ddH₂O to three different levels: 10¹, 10² and 10³. These yeast cells were challenged with multiple abiotic stresses to evaluate their performance. Then 5 µL of each culture was separately spotted onto SD-U solid medium plates plus different reagents, including 0 M reagent, 1.8 M sodium chloride (NaCl), 2.0 M potassium chloride (KCl), and 4.0 M sorbitol. The plates were incubated at 29 °C for 10 d and then photographed.

Transcriptome data validation using RT-qPCR

The RNAprep Pure Plant Plus Kit (Polysaccharides & Polyphenolics-rich) (TIANGEN) was used to isolate total RNA from roots, stems, leaves, and apical buds under salt stress in *P. alba* and the PrimeScript™ RT reagent kit (Perfect Real Time) (TaKaRa, Dalian, China) was used for reverse transcription. Three DEGs were selected for validation with quantitative real-time polymerase chain reaction (RT-qPCR), using the conserved ACTIN (GenBank no. PP754761) as a reference gene. Using the cDNA strand of each sample as a template, PCR amplification was carried out in the PrimerScript RT Reagent Kit (Perfect Real Time, Takara) on a LightCycler® 480 II instrument (Roche Diagnostics, Indianapolis, USA) using specific primers (Table S6). Relative expression levels were calculated using the $2^{-\Delta\Delta CT}$ method [54]. Three independent biological replicates and four technical replicates were analyzed in this experiment.

Statistical analysis

Independent sample *t*-test were carried out for comparing the data between control and salt stress groups in SPSS v24 software. Significant differences at $P < 0.05$ and $P < 0.01$ were indicated using * and **, respectively.

Declarations

Acknowledgements

We would like to acknowledge the contributions of Wei Fan and Shuai Liu (State Key Laboratory of Tree Genetics and Breeding, Chinese Academy of Forestry, Beijing) for their technical assistance in ICP-MS analysis.

Author contributions

X.Y.B. performed the experiments, data analysis and wrote the original draft. Y.X. and P.F.J. provided valuable suggestions for the experiments. Q.Y.Z. and Y.J.L. designed the experiments and wrote the manuscript.

Funding

This study was supported by National Key R&D Program of China (2022YFD2200102) and the Chinese Academy of Forestry (TGB2022001 and TGBFRF202301).

Availability of data and materials

The sequenced raw reads have been submitted to the National Center for Biotechnology Information (NCBI) with BioProject ID: PRJNA1107006. The cloned sequences have been deposited in GenBank no. PP754731~PP754760. All data generated or analyzed during this study are included in this published article and its supplementary information files.

Ethics approval and consent to participate

Not applicable.

Consent for publication

Not applicable.

Competing interests

The authors declare no competing interests.

References

1. van Zelm E, Zhang Y, Testerink C. Salt tolerance mechanisms of plants. *Annu Rev Plant Biol.* 2020; 71(1): 403-433.
2. Zhang HM, Zhu JH, Gong ZZ, Zhu JK. Abiotic stress responses in plants. *Nat Rev Genet.* 2022; 23(2): 104-119.
3. Rengasamy P. World salinization with emphasis on Australia. *J Exp Bot.* 2006; 57(5): 1017-1023.
4. Zhao CZ, Jiang W, Zayed O, Liu X, Tang K, Nie WF, et al. The LRXs-RALFs-FER module controls plant growth and salt stress responses by modulating multiple plant hormones. *National Sci Rev.* 2021; 8(1): nwaa149.
5. Yu ZP, Duan XB, Luo L, Dai SJ, Ding ZJ, Xia GM. How plant hormones mediate salt stress responses. *Trends Plant Sci.* 2020; 25(11): 1117-1130.
6. Munns R, Tester M. Mechanisms of salinity tolerance. *Annual Review of Plant Biology.* 2008; 59(1): 651-681.
7. Sudhir P, Murthy SDS. Effects of salt stress on basic processes of photosynthesis. *Photosynthetica.* 2004; 42(2): 481-486.
8. Galvan-Ampudia CS, Testerink C. Salt stress signals shape the plant root. *Curr Opin Plant Biol.* 2011; 14(3): 296-302.
9. Flowers TJ, Munns R, Colmer TD. Sodium chloride toxicity and the cellular basis of salt tolerance in halophytes. *Ann Bot.* 2014; 115(3): 419-431.
10. Tabassum A, Akram S, Mushtaq M. Chapter 11-Apiole. a centum of valuable plant bioactives. Academic Press. 2021; p233-259.
11. Horie T, Karahara I, Katsuhara M. Salinity tolerance mechanisms in glycophytes: An overview with the central focus on rice plants. *Rice (N Y).* 2012; 5(1):11.
12. Brundu G, Lupi R, Zapelli I, Fossati T, Patrignani G, Camarda I, et al. The origin of clonal diversity and structure of *Populus alba* in sardinia: evidence from nuclear and plastid microsatellite markers. *Ann Bot.* 2008; 102(6): 997-1006.

13. Goikoetxea PG, Agundez D. Oaks and beeches in Spain. Genetic resources conservation. Forest Syst. 2000; 9(4) :125-142.
14. Wei TT, Ma YD, Zheng FM. The present situation and comprehensive treatment of soil salinization in Xinjiang (in Chinese with English abstract). Anhui Agri Sci Bull. 2020; 26(10):107-110.
15. Miller G, Suzuki N, Ciftci-Yilmaz S, Mittler R. Reactive oxygen species homeostasis and signalling during drought and salinity stresses. Plant Cell Environ. 2010; 33(4): 453-467.
16. Zhao HM, Zheng DF, Feng NJ, Zhou GS, Khan A, Lu XT, et al. Regulatory effects of hemin on prevention and rescue of salt stress in rapeseed (*Brassica napus L.*) seedlings. BMC Plant Biol. 2023; 23(1): 558.
17. Gill SS, Tuteja N. Reactive oxygen species and antioxidant machinery in abiotic stress tolerance in crop plants. Plant Physiol Biochem. 2010; 48(12): 909-930.
18. Guo Q, Liu L, Rupasinghe TWT, Roessner U, Barkla BJ. Salt stress alters membrane lipid content and lipid biosynthesis pathways in the plasma membrane and tonoplast. Plant Physiol. 2022; 189(2): 805-826.
19. Awasthi JP, Saha B, Chowdhara B, Devi SS, Borgohain P, Panda SK. Qualitative analysis of lipid peroxidation in plants under multiple stress through schiff's reagent: a histochemical approach. Bio Protoc. 2018; 8(8): e2807.
20. Hu DD, Li RF, Dong ST, Zhang JW, Zhao B, Ren BZ, et al. Maize (*Zea mays L.*) responses to salt stress in terms of root anatomy, respiration and antioxidative enzyme activity. BMC Plant Biol. 2022; 22(1): 602.
21. Adil M, Bashir S, Bashir S, Aslam Z, Ahmad N, Younas T, et al. Zinc oxide nanoparticles improved chlorophyll contents, physical parameters, and wheat yield under salt stress. Front Plant Sci. 2022; 13: 932861.
22. Meng FY, Feng NJ, Zheng DF, Liu ML, Zhang RJ, Huang XX, et al. Exogenous Hemin alleviates NaCl stress by promoting photosynthesis and carbon metabolism in rice seedlings. Sci Rep. 2023; 13(1): 3497.
23. Zhu JK. Salt and drought stress signal transduction in plants. Annu Rev Plant Biol. 2002; 53: 247-273.
24. Niu ML, Xie JJ, Chen C, Cao HS, Sun JY, Kong QS, et al. An early ABA-induced stomatal closure, Na^+ sequestration in leaf vein and K^+ retention in mesophyll confer salt tissue tolerance in *Cucurbita* species. J Exp Bot. 2018; 69(20): 4945-4960.
25. Papon N, Courdavault V. ARResting cytokinin signaling for salt-stress tolerance. Plant Sci. 2022; 314: 111116.
26. Yu Y, Li YL, Yan ZW, Duan XB. The role of cytokinins in plant under salt stress. J Plant Growth Regul. 2021; 41: 2279-2291.
27. Ahmad B, Mukarram M, Choudhary S, Petrík P, Dar TA, Khan MMA. Adaptive responses of nitric oxide (NO) and its intricate dialogue with phytohormones during salinity stress. Plant Physiol Biochem.

2024; 208: 108504.

28. Zhang XC, Hu JP. FISSION1A and FISSION1B proteins mediate the fission of peroxisomes and mitochondria in *Arabidopsis*. *Mol Plant*. 2008; 1(6): 1036-1047.
29. Frick EM, Strader LC. Kinase MPK17 and the peroxisome division factor PMD1 influence salt-induced peroxisome proliferation. *Plant Physiol*. 2017; 176(1): 340-351.
30. Xu Y, Tie WW, Yan Y, Xu BY, Liu JH, Li MY, et al. Identification and expression of the BAHD family during development, ripening, and stress response in banana. *Mol Biol Rep*. 2021; 48(2): 1127-1138.
31. Hao XY, Wang B, Wang L, Zeng JM, Yang YJ, Wang XC. Comprehensive transcriptome analysis reveals common and specific genes and pathways involved in cold acclimation and cold stress in tea plant leaves. *Sci Hortic*. 2018; 240: 354-368.
32. Molina I, Kosma D. Role of HXXXD-motif/BAHD acyltransferases in the biosynthesis of extracellular lipids. *Plant Cell Rep*. 2015; 34: 587-601.
33. D'Auria JC. Acyltransferases in plants: a good time to be BAHD. *Curr Opin Plant Biol*. 2006; 9(3): 331-340.
34. Torrens-Spence MP, Bobokalonova A, Carballo V, Glinkerman CM, Pluskal T, Shen A, et al. PBS3 and EPS1 complete salicylic acid biosynthesis from isochorismate in *Arabidopsis*. *Mol Plant*. 2019; 12(12):1577-1586.
35. Gautam T, Dutta M, Jaiswal V, Zinta G, Gahlaut V, Kumar S. Emerging roles of SWEET sugar transporters in plant development and abiotic stress responses. *Cells*. 2022; 11(8): 1303.
36. Seo PJ, Park JM, Kang SK, Kim SG, Park CM. An *Arabidopsis* senescence-associated protein SAG29 regulates cell viability under high salinity. *Planta*. 2011; 233(1): 189-200.
37. Steponkus PL, Lanphear FO. Refinement of the triphenyl tetrazolium chloride method of determining cold injury. *Plant Physiol*. 1967; 42(10): 1423-1426.
38. Yang Q, Blanco NE, Hermida-Carrera C, Lehotai N, Hurry V, Strand Å. Two dominant boreal conifers use contrasting mechanisms to reactivate photosynthesis in the spring. *Nat Commun*. 2020; 11(1): 128.
39. Bruijnsma J. The quantitative analysis of chlorophylls a and b in plant extracts. *Photochem Photobiol*. 1963; 2(2): 241-249.
40. Chen SF, Zhou YQ, Chen YR, Gu J. fastp: an ultra-fast all-in-one FASTQ preprocessor. *Bioinformatics*. 2018; 34(17): i884-i890.
41. Kim D, Paggi JM, Park C, Bennett C, Salzberg SL. Graph-based genome alignment and genotyping with HISAT2 and HISAT-genotype. *Nat Biotechnol*. 2019; 37(8): 907-915.
42. Pertea M, Kim D, Pertea GM, Leek JT, Salzberg SL. Transcript-level expression analysis of RNA-seq experiments with HISAT, StringTie and Ballgown. *Nat Protoc*. 2016; 11(9): 1650-1667.
43. Love MI, Huber W, Anders S. Moderated estimation of fold change and dispersion for RNA-seq data with DESeq2. *Genome Biol*. 2014; 15(12): 550.

44. Benjamini Y, Yekutieli D. The control of the false discovery rate in multiple testing under dependency. *Ann Stat.* 2001; 29(4): 1165-1188.
45. Ginetet C. ggplot2: elegant graphics for data analysis. *J R Stat Soc Ser A Stat Soc.* 2011; 174(1): 245-246.
46. Ernst J, Bar-Joseph Z. STEM: a tool for the analysis of short time series gene expression data. *BMC Bioinformatics.* 2006; 7(1): 191.
47. Yu GC, Wang LG, Han YY, He QY. clusterProfiler: an R package for comparing biological themes among gene clusters. *OMICS.* 2012; 16(5): 284-287.
48. Xu C, Gao M, Zhang JH, Fu YF. IL5RA as an immunogenic cell death-related predictor in progression and therapeutic response of multiple myeloma. *Sci Rep.* 2023; 13(1): 8528.
49. Goodstein DM, Shu SQ, Howson R, Neupane R, Hayes RD, Fazo J, et al. Phytozome: a comparative platform for green plant genomics. *Nucleic Acids Res.* 2012; 40(D1): D1178-D1186.
50. Katoh K, Misawa K, Kuma KI, Miyata T. MAFFT: a novel method for rapid multiple sequence alignment based on fast fourier transform. *Nucleic Acids Res.* 2002; 30(14): 3059-3066.
51. Minh BQ, Schmidt HA, Chernomor O, Schrempf D, Woodhams MD, Haeseler A, et al. IQ-TREE 2: new models and efficient methods for phylogenetic inference in the genomic era. *Mol Biol Evol.* 2020; 37(5): 1530-1534.
52. Langfelder P, Horvath S. WGCNA: an R package for weighted correlation network analysis. *BMC Bioinformatics.* 2008; 9: 559.
53. Hu Z. Using VisANT to analyze networks. *Curr Protoc Bioinformatics.* 2014; 45(88): 8.8.1-8.8.39.
54. Pfaffl MW. A new mathematical model for relative quantification in real-time RT-PCR. *Nucleic Acids Res.* 2001; 29(9): e45.

Figures

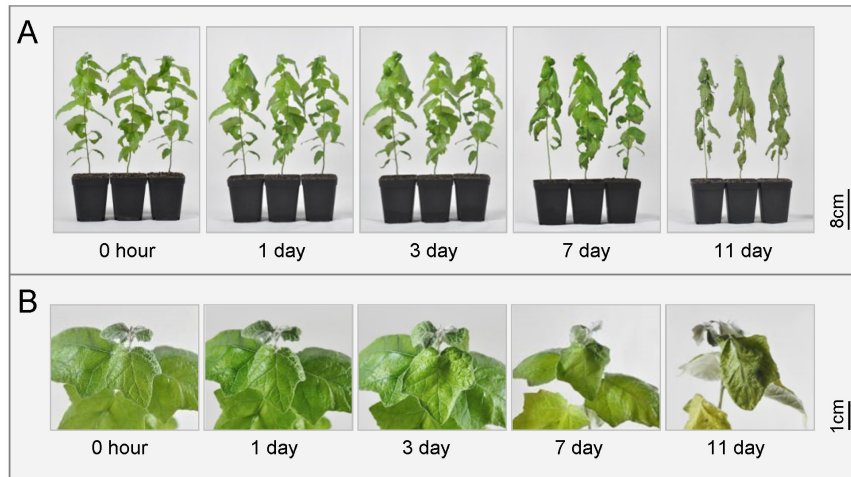


Fig. 1 Phenotypes of whole plant (A) and leaves (B) of *P. alba* seedlings under salt stress.

Figure 1

See image above for figure legend

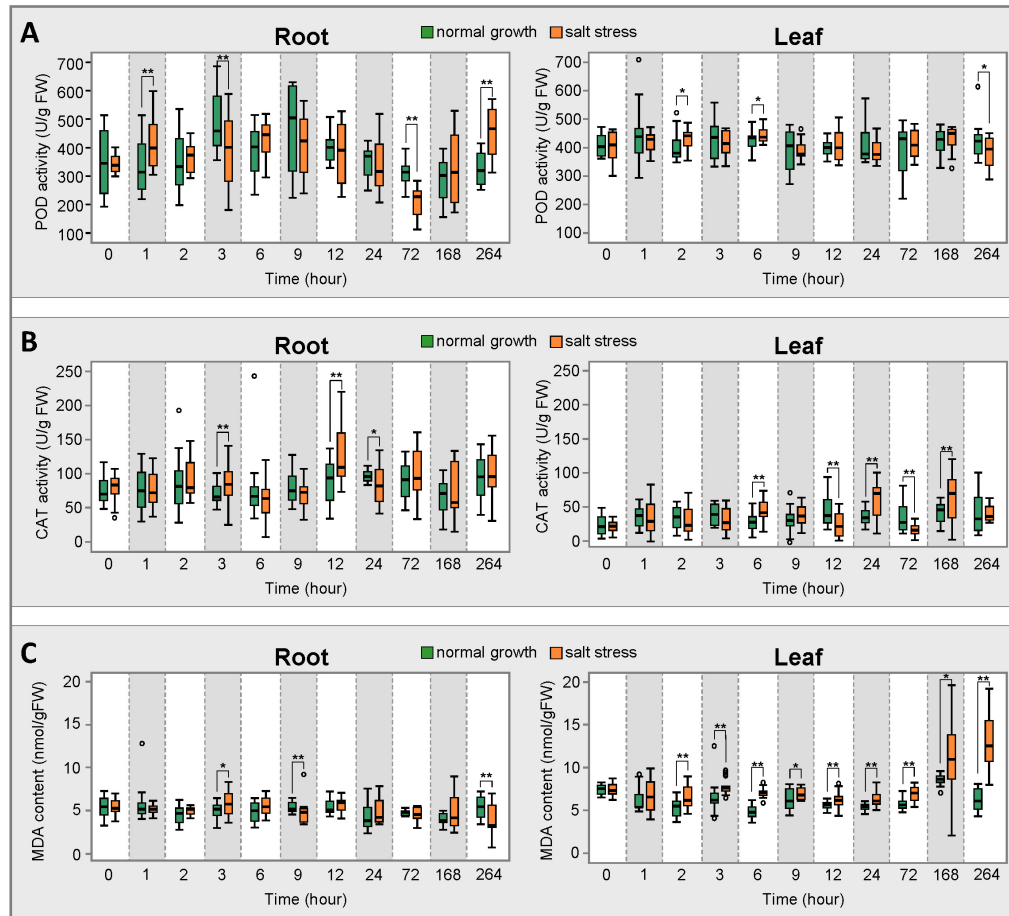


Fig. 2 POD activity (A), CAT activity (B) and MDA content (C) in roots and leaves of *P. alba* seedlings under salt stress. *, $P<0.05$; **, $P<0.01$.

Figure 2

See image above for figure legend

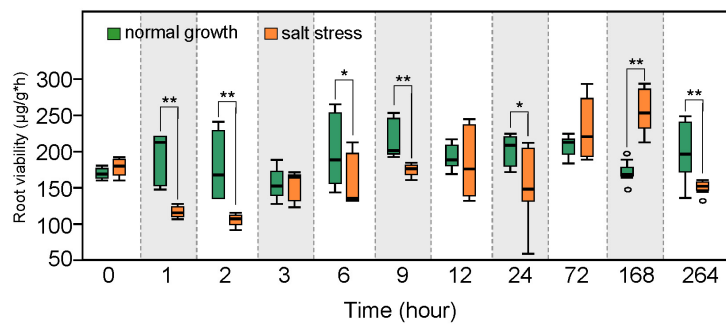


Fig. 3 Root viability of *P. alba* seedlings under salt stress. *, $P<0.05$; **, $P<0.01$.

Figure 3

See image above for figure legend

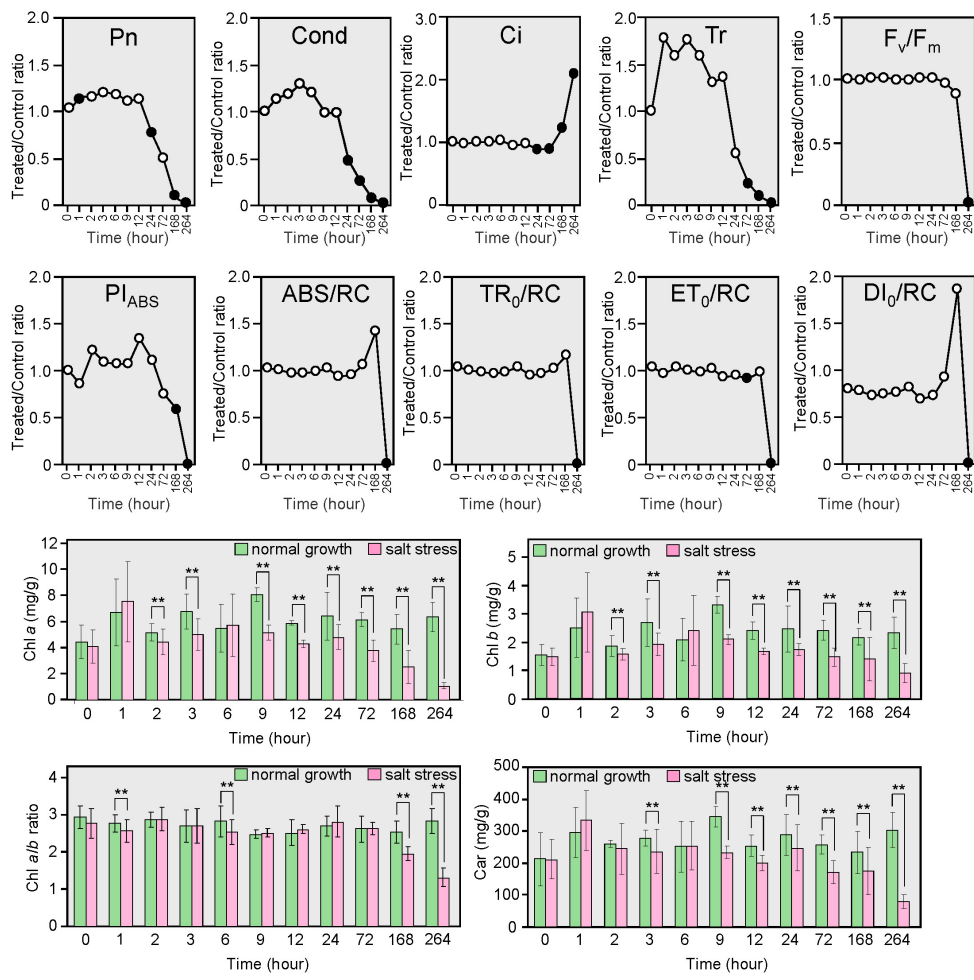


Fig. 4 Photosynthetic parameters of *P. alba* seedlings under normal growth conditions and salt stress. Pn, net photosynthetic rate; Cond, stomatal conductance; Ci, intercellular CO_2 concentration; Tr, transpiration rate; F_v/F_m , maximum quantum efficiency of photosystem II (PSII) photochemistry; PI_{ABS} , performance index (potential) for energy conservation from photons absorbed by PSII to the reduction of intersystem electron acceptors; ABS/RC, maximal energy fluxes for absorption per reaction center; TR_0/RC , maximal energy fluxes for trapping per reaction center; ET_0/RC , maximal energy fluxes for electron transport rate per reaction center; DI_0/RC , maximal energy fluxes for energy dissipation per reaction center; Chl a , chlorophyll a ; Chl b , chlorophyll b ; Car, carotenoid. Solid black dot represented the significant difference between control and treated groups. *, $P < 0.05$; **, $P < 0.01$.

Figure 4

See image above for figure legend

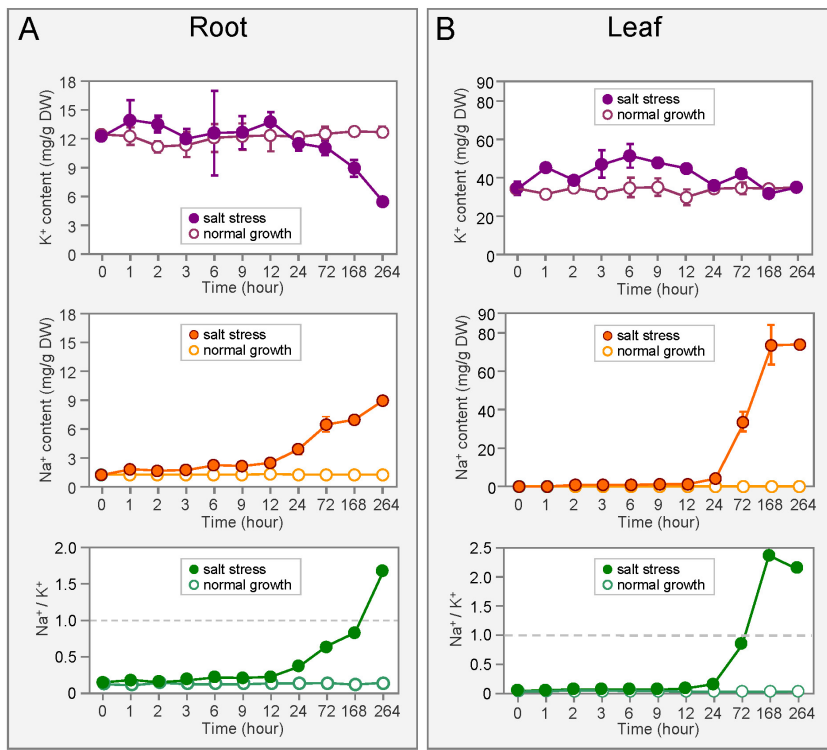


Fig. 5 Contents of potassium and sodium ions in roots (A) and leaves (B) of *P. alba* under normal growth conditions and salt stress.

Figure 5

See image above for figure legend

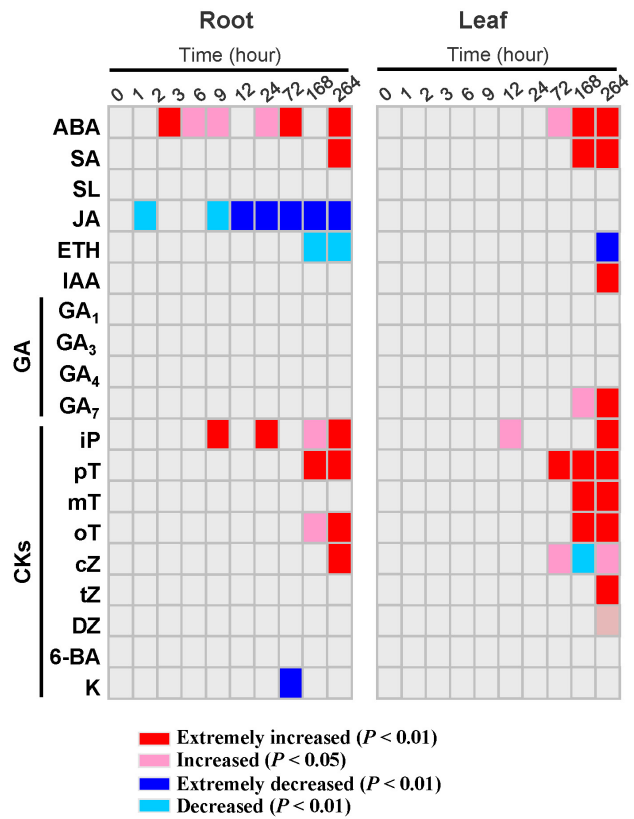


Fig. 6 Hormone content in roots and leaves of *P. alba* under salt stress. ABA, abscisic acid; SA, salicylic acid; SL, strigolactone; JA, jasmonic acid; ETH, ethylene; IAA, indole acetic acid; GA₁, gibberellin A₁; GA₃, gibberellin A₃; GA₄, gibberellin A₄; GA₇, gibberellin A₇; iP, N⁶-(Δ^2 -isopentenyl)-adenine; pT, para-Topolin; mT, meta-Topolin; oT, ortho-Topolin; cZ, cis-Zeatin; tZ, trans-Zeatin; DZ, dihydrozeatin; 6-BA, 6-benzyladenine; K, kinetin.

Figure 6

See image above for figure legend

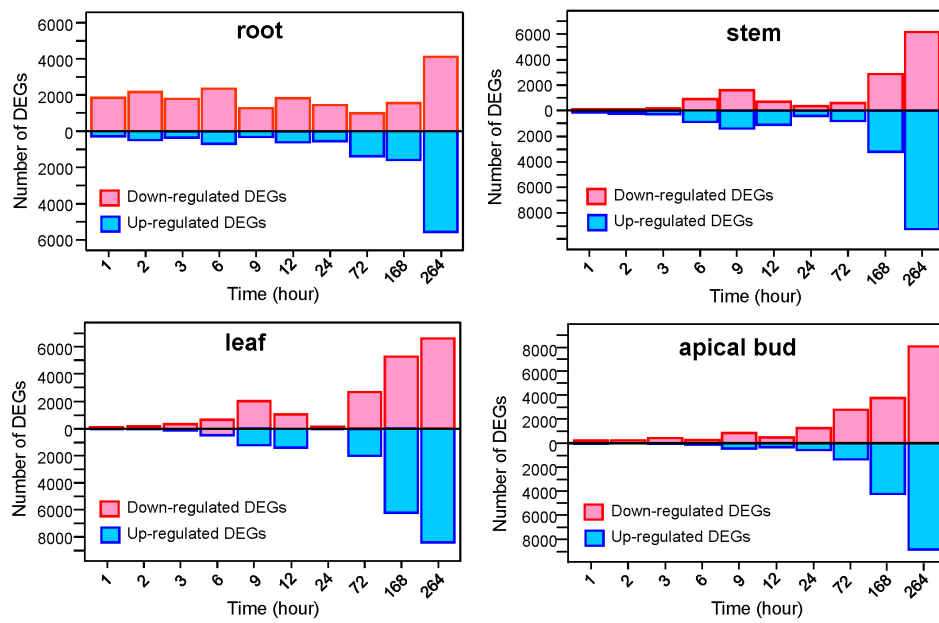


Fig. 7 Differentially expressed genes (DEGs) in roots, stems, leaves, and apical buds of *P. alba* under salt stress.

Figure 7

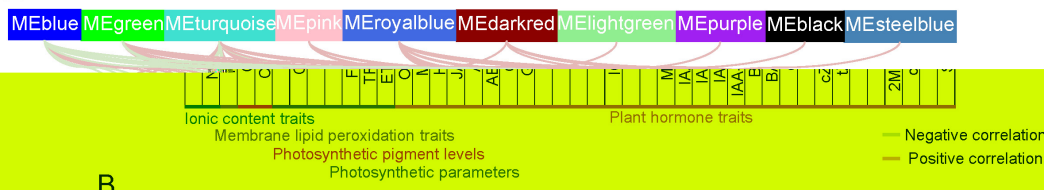
See image above for figure legend



Figure 8

See image above for figure legend

A



B

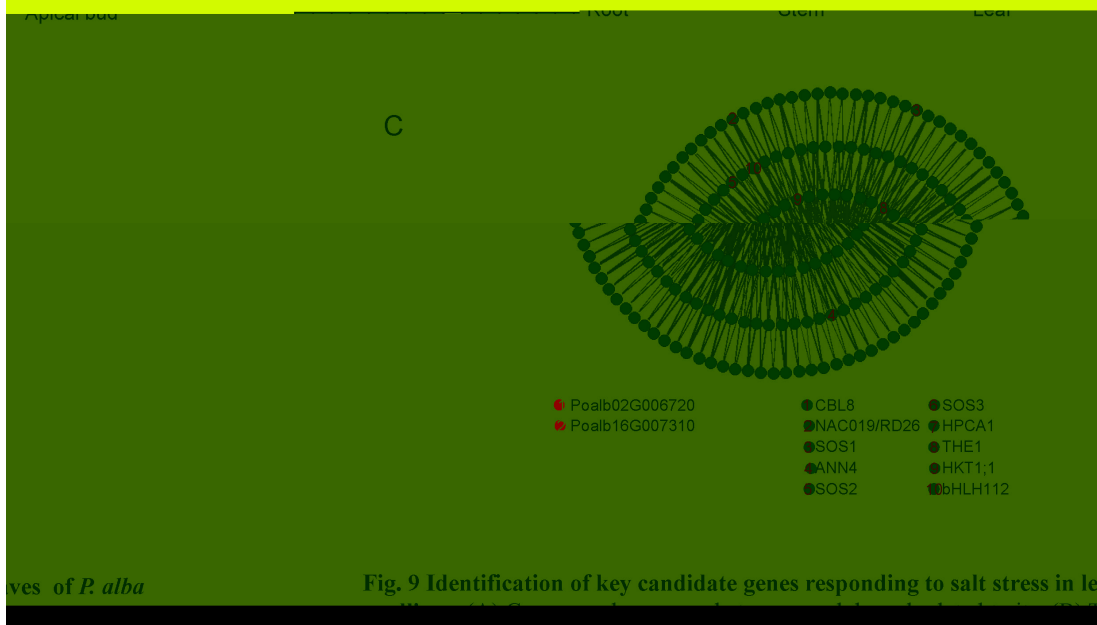


Fig. 9 Identification of key candidate genes responding to salt stress in leaves of *P. alba*

Figure 9

See image above for figure legend

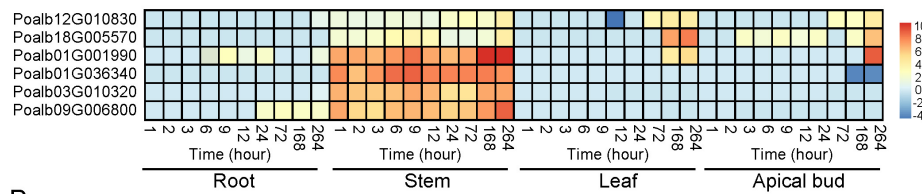
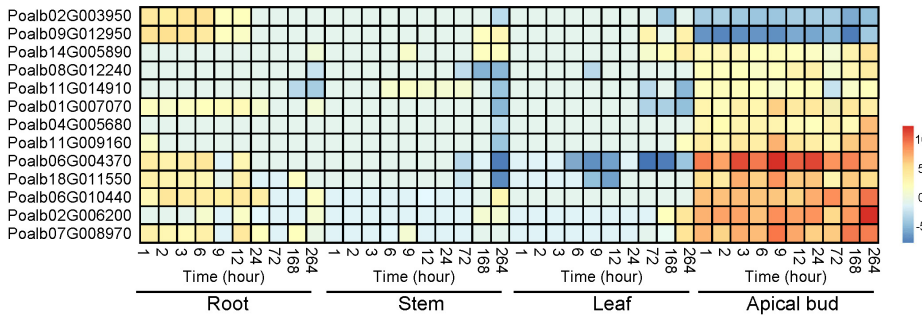
A**B**

Fig. 10 The expression patterns of key candidate genes in response to salt stress in stems (A) and apical buds (B) of *P. alba* seedlings.

Figure 10

See image above for figure legend



Fig. 11 Functional verification of key candidate genes of *P. alba* responding to salt stress.

Figure 11

See image above for figure legend

Supplementary Files

This is a list of supplementary files associated with this preprint. Click to download.

- Additionalfile1.xls
- AdditionalFile2.pdf